

# The Microstructure of Concrete

KAREN L. SCRIVENER, Imperial College

*The great tragedy of science: the slaying of a  
beautiful hypothesis by an ugly fact.*

Thomas Huxley

The various aspects which contribute to the microstructure of concrete are considered and illustrated, from the microstructure of the anhydrous cement to the microstructure of mature concrete. At each stage the importance of quantitative characterization and methods of achieving this are discussed.

## Introduction

At some level the behavior of every material is related to its microstructure. The understanding of these relationships between structure and properties forms the basis of materials science. Microstructure encompasses a wide range of structural levels, from the atomic scale to that of the engineering component, and includes all discontinuities inside and between phases, such as dislocations, grain boundaries, phase interfaces, pores, and cracks.<sup>1</sup> A complete characterization of the microstructure of a multiphase material must also entail quantitative information about the relative proportions of the phases and their distribution in space. The relative lack of success in developing microstructure/property relationships for concrete is due, in no small part, to the lack of good microstructural characterization.

In microstructural terms, concrete is an extremely complex system of solid phases, pores, and water, with a high degree of heterogeneity. This heterogeneity can be considered on several levels. At the simplest level, concrete consists of aggregate particles, distributed in a matrix of cement paste. On a more detailed level, the paste itself is a mixture of unreacted cement, hydration products, pores, and water and at a still finer level these phases themselves have complex microstructures.

In this chapter, various aspects of the microstructure of concrete will be considered in an attempt to provide a coherent picture. As an introduction, a brief description of the chemistry and structure of the solid phases in cement pastes is given, followed by a short survey of the physical methods used to study microstructure. Initially, the components of the concrete microstructure are considered separately: the microstructure of anhydrous cement; the development of microstructure during the hydration of cement paste; the microstructure of

aggregates; and the interface between cement paste and aggregates. To arrive at a complete characterization of concrete microstructure, these components must be integrated, but this is an area in which much work needs to be done and only a few comments can be made. For conciseness, it has been possible to cover only the microstructural development of concretes at near ambient temperatures.

## Solid Phases in Cement Paste

Anhydrous cement powder is a combination of oxides of calcium, silicon, aluminum, and iron (plus small amounts of other oxides). The four principal minerals found in ordinary portland cement are alite, impure tricalcium silicate ( $C_3S$ ); belite, impure dicalcium silicate ( $C_2S$ ); and the aluminate and ferrite phases which have average compositions of  $C_3A$  and  $C_4AF$ , respectively. These minerals react with water to give a variety of hydrates. The calcium silicates react to give calcium hydroxide and calcium silicate hydrate and the aluminate and ferrite phases react with the added calcium sulfate to give two groups of product referred to as AFt and AFm.

Calcium hydroxide (CH) is the only hydration product to have a well-defined stoichiometry and crystal structure and normally forms as massive, relatively pure crystals with a euhedral hexagonal habit.

The calcium silicate hydrate in cement paste is a gel which shows no long-range crystallinity. Its composition is uncertain (and possibly variable) with a C/S ratio of about 1.7 to 2.0; consequently it is usually written as C-S-H. The short-range order of this phase is probably related to the layer structure of the crystalline calcium silicate hydrates—1.4 nm tobermorite ( $C_5S_6H_9$ ) and jennite ( $C_6S_6H_{11}$ ).<sup>2,3</sup> This phase appears to adopt a wide range of morphologies,<sup>4-6</sup> some based on thin sheets which may give fibrillar or honeycomb structures at early ages, others with a more compact structure forming at later ages.

The term AFt denotes the phases related to ettringite—calcium aluminum trisulfate ( $C_3A \cdot 3CS \cdot 32H_2O$ ) with the F indicating the possible substitution of iron for aluminum in the structure. This phase forms when the concentration of sulfate ions in solution is relatively high and has a morphology of hexagonal rods.

The AFm phases are isostructural with calcium aluminum monosulfate ( $C_3A \cdot CS \cdot 12H_2O$ ). In addition to possible substitution of aluminum by iron, hydroxide, carbonate, or chloride ions may replace the sulfate. These phases have a hexagonal plate morphology.

## Techniques for Studying Microstructure

There are many techniques which have been used to study microstructure; they can be divided broadly into two categories. Indirect or bulk techniques give information on average features of the whole microstructure. Examples of indirect techniques are thermogravimetry (TG) and X-ray diffraction (XRD), which can be used to determine the amounts of certain phases in the sample. Methods used to obtain information about the pore-size distribution, such as mercury intrusion porosimetry (MIP) and methanol absorption, are also indirect techniques as they give no information as to how the pores are arranged in space. The other group of techniques is direct or microscopical techniques which provide information about the way in which the component phases are arranged in the microstructure.

The advantage of the indirect techniques is that they provide information in a quantitative form so that different samples can be compared objectively. In contrast, information derived from direct techniques usually takes the form of images. Images are extremely valuable in conveying a vivid impression of the microstructure, but comparisons between different samples are more subjective and rely on the experience and interpretation of the observer. As most of the findings presented here have been obtained by microscopy techniques, their application to the study of the microstructure of cement and concrete will be discussed in more detail.

Optical microscopy has been widely used in the study of cement and concrete.<sup>7</sup> The use of suitable etchants makes it possible to study the distribution of anhydrous phases in clinker and cement powder.<sup>8,9</sup> In hydrated pastes and concrete there is little contrast between the phases in reflected light. However, in thin sections the refractive properties of different phases and the use of fluorescent resin can indicate cement and aggregate type, the presence of mineral admixtures, the w/c ratio, the quality of compaction, and the presence of alkali silica reaction (e.g., Refs. 10 and 11).

Ultimately, the resolution of optical microscopy is limited by the wavelength of light and for detailed microstructural studies electron microscopy must be used. As cement is nonconducting, and due to the presence of water, the preparation of cement pastes and concretes for electron microscopy poses problems. The possible effects of drying on the microstructure and the selectivity of different preparation techniques must be considered when interpreting electron micrographs of cement pastes.

Fracture surfaces provide a relatively simple means to observe the three-dimensional arrangement of hydration products. These surfaces can be imaged by secondary electrons in the scanning electron microscope with fairly good resolution ( $\approx 10$  nm). While providing much useful information, the microstructure observed using this technique is that of cement paste which has been dried and exposed to the high vacuum of the electron microscope. Given the amorphous nature of the hydration products, it is likely that some alteration in their morphology will occur during specimen preparation. Also, only fracture paths are revealed, so that weak areas of the microstructure predominate. In young pastes the fracture path is interparticular, showing only the outer surface of the hydration products. In older pastes the fracture surface is dominated by areas of cleaved calcium hydroxide, which has grown in the originally water-filled space to engulf the other hydration products. After hydration for longer than one day it becomes increasingly difficult to assess the extent to which fracture surfaces are representative of the bulk microstructure.

Undried cement pastes can be examined if the area around the specimen can be isolated from the high vacuum in the electron microscope column. In the AEI EM7 1 MeV high-voltage electron microscope (HVEM) there is a comparatively large space between the objective pole pieces, which permits the incorporation of an environmental cell. Two types of environmental cell have been used to study the hydration of cement in the HVEM. Double and coworkers<sup>12,13</sup> have studied the hydration of cement in a window-type cell, at a high water/cement ratio. With this type of cell, the resolution is limited by the presence of windows and further by the large excess of water in the paste. The cell used by Jennings and Pratt<sup>14</sup> and by Scrivener<sup>6</sup> and Scrivener and Pratt<sup>15</sup> has pairs of differentially pumped open apertures. Pressures of up to 300  $\tau$  can be maintained in the cell with water-saturated gases and better resolution can be obtained than with the window-type cell. Using this technique, much information can be gained on the morphology of

hydration products in the undried state and the way in which their morphology changes on drying. However, due to the method of specimen preparation it is still only the outer surfaces of the hydrating grains which can be observed.

Ion-beam thinned sections allow the structure to be viewed in cross section in the transmission electron microscope.<sup>6,15-20</sup> The brittleness of cement pastes and concretes makes the preparation of electron-transparent sections by ion-beam thinning very difficult and young pastes must first be impregnated with epoxy resin. The use of scanning transmission electron microscopy (STEM) minimizes damage to the cement by the electron beam. Fairly extensive electron-transparent areas can be obtained with careful thinning; nevertheless a certain amount of selectivity is inevitable.

Another technique uses backscattered electron images of polished sections. With thick polished sections, large cross-sectional areas can be observed by SEM. However, they do not show good secondary electron contrast. Using a pair of backscattered electron (bse) detectors, images can be produced in which the intensity is dependent on the average atomic number of the scanned area. Thus, in polished unetched sections the anhydrous material, massive calcium hydroxide, other hydration products, porosity, and aggregate particles can be distinguished from one another.<sup>6,21</sup> The contrast between these constituents is sufficient to allow quantitative image analysis of their total area and size distribution.<sup>22</sup> The form and distribution of the hydration products observable is comparable with, though of lower resolution than, that seen in the STEM of thin foils. However, bse images may be taken over a large cross-sectional area, eliminating the selectivity of ion-beam thinning used to prepare STEM specimens.

## Microstructure of Anhydrous Cement

An account of the microstructural development of concrete must start by considering the microstructure of the starting materials. The microstructure of the most important of these, anhydrous cement, is determined by the microstructure of the clinker produced in cement kiln and the way in which the clinker breaks up during grinding. The resulting product is quite different, in both appearance and reactivity, from a simple mixture of monomineralic grains of the four main anhydrous minerals.

An "ideal" clinker microstructure consists of crystals of alite and belite (which are solid at the firing temperature) in a matrix of interstitial phases which solidify from the melt during cooling. The alite crystals have a hexagonal habit, while the belite crystals tend to be rounded. In the interstitial material, the aluminate and ferrite phases may be finely divided and intergrown. The details of the microstructure, such as the shape and distribution of the phases, will depend on the physical and chemical characteristics of the raw mix (fineness, homogeneity, and chemical composition) and the exact conditions of burning and cooling of the clinker. Nevertheless, the general features described above can be identified in most commercial clinkers, such as that shown in Fig. 1. This clinker also shows extensive cracking, which commonly occurs due to thermal stresses during cooling.

Clinker is ground with gypsum to give a powder with a wide range of particle sizes from less than 1  $\mu\text{m}$  to about 100  $\mu\text{m}$ . Secondary electron images of cement powder by SEM (Fig. 2) give some impression of this size distribution and show the agglomeration of many smaller grains on the surface of the larger grains. Such images also reveal fine particles of gypsum spread over the grain surfaces.



**Fig. 1.** Microstructure of a commercial clinker (bse image). Light-gray crystals of alite and darker rounded crystals of belite can be seen in a matrix of the interstitial phases—ferrite (light) and aluminate (darker). Porosity (black) can also be seen.

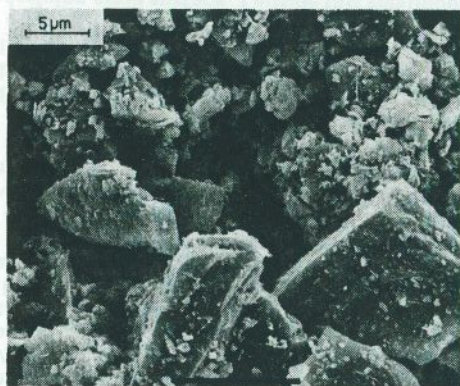


**Fig. 2.** Scanning electron micrograph of anhydrous cement grains showing the wide range of particle sizes. Small lathlike crystals of calcium sulfate can be seen on the surfaces of the larger grains.

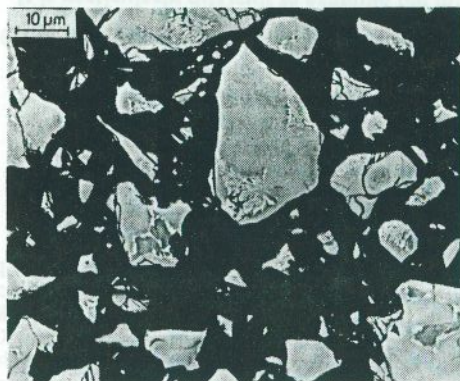


**Fig. 3.** Backscattered electron image of polished section of anhydrous cement grains dispersed in resin. It can be seen that most of the grains are polymineralic.

The distribution of phases within the cement grains can be studied in polished sections prepared from samples of cement dispersed in epoxy resin. Examination of such sections with backscattered electrons by SEM (Fig. 3) indicates that fracture through the alite crystals dominates the grinding process, with little evidence of fracture along the interphase boundaries. Almost all grains larger than 2 to 3  $\mu\text{m}$  are polymineralic and on the surfaces of the larger grains only small areas of interstitial materials are exposed, between areas of alite. Relatively greater proportions of aluminate and ferrite phases are exposed on the surface of smaller grains, as their formation is more likely to involve fracture through the interstitial material.

At present, most cements are characterized solely by their surface area and oxide composition. The surface area is generally determined by permeability methods. Such methods give a much lower value for the surface area than absorption methods (such as BET), because blocked channels are not accessible to the moving air stream. Surface area measurements give little information about the particle-size distribution, which is of great importance in determining the packing of the cement grains in paste and concrete. Laser diffraction methods can be used to measure the size distribution; the result for a typical cement is shown in Fig. 4.

From the oxide composition, the Bogue calculation<sup>23</sup> may be used to estimate the relative proportions of the major phases. This calculation assumes that complete reaction occurs in the kiln and takes no account of any solid solution between the phases or of the presence of minor oxides, and may give quite inaccurate results. Quantitative X-ray diffraction can be used to measure the proportions of the clinker phases<sup>24-26</sup> and accuracies of 1% are claimed for this method if a suitable range of standards is used.<sup>26</sup> Analyses of clinker can also be obtained by optical microscopy using a point-counting method on polished and etched sections of clinker.

As illustrated in Fig. 3, the distribution of phases within the cement grains can be seen in bse images of polished sections. If these images are analyzed in conjunction with dot maps from energy dispersive X-ray analyses of the same areas, the relative amounts of silicate and interstitial phases can be measured.<sup>27</sup> This technique can be extended to assess the relative proportions of the phases exposed on the surfaces of the grains, which might be expected to determine the initial reactivity of the cement. Preliminary studies have shown that these surface proportions may differ significantly from the bulk values. Other studies using secondary ion mass spectroscopy (SIMS) have shown that the surfaces of the cement grains may contain high proportions of impurities,<sup>28</sup> which might also affect the reactivity.

Proper characterization of anhydrous cement is an important first step in understanding differences in the reactivity of cements and the properties of the concretes made from them.

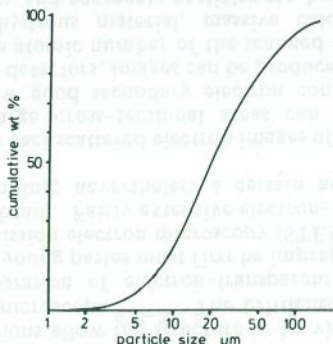


Fig. 4. Particle-size distribution for a typical cement obtained by laser diffraction.

## Development of Microstructure During Hydration of Cement Paste

During hydration, cement paste changes from a fluid mixture of cement powder and water to a rigid solid. The reactions which occur are exothermic and the overall progress of the reaction can be studied by isothermal conduction calorimetry. From a typical rate-of-heat-evolution curve for an ordinary portland cement, various stages of hydration can be identified, which will be used as a basis for describing the microstructural development (the times indicated are intended only as a general guide and will be affected by a variety of factors including temperature and admixtures):

- I (about 0 to 3 hours). On mixing, a large amount of heat is evolved; the rate of heat evolution then decreases rapidly to a minimum after about 3 hours. This initial period, during which the cement remains fluid and workable, is often referred to as the induction period.
- II (about 3 to 24 hours). During this period some 30% of hydration occurs, which is reflected by the major peak in the rate of heat evolution.
- III (24 hours onward). After about 24 hours the rate of heat evolution declines, although hydration may continue indefinitely.

### I (0 to 3 Hours)

It is particularly difficult to examine the microstructure of cement paste during this period. Most of the mixing water is present as free water. If this water is removed so that specimens can be examined in the electron microscope, fundamental changes in the microstructure may occur. Even apart from any damage caused by drying, the time taken for specimen preparation makes it difficult to follow the progress of the hydration accurately. These problems make examination of specimens without prior drying, in the environmental cell of the HVEM, an especially valuable technique for studying the early hydration. Using this technique, specimens can be examined as little as 10 minutes after mixing.

Several workers have reported the appearance of a gelatinous layer on the surface of cement soon after mixing.<sup>6,13,14,29</sup> Micrographs of undried cement taken in the environmental cell (Fig. 5) show an indistinct layer of product on the surface.<sup>30</sup> Similar early product has been observed during the hydration of  $C_3A$  with gypsum.<sup>30</sup> In the hydration of  $C_3S$ , the early formation of product has also been noted,<sup>6,31</sup> but in this case the product appears to have a somewhat different morphology of exfoliating films. Considering the polymineralic nature of cement grains, the gelatinous layer observed in the hydration of cement is probably an amorphous colloidal product, rich in alumina and silica, but also containing significant amounts of calcium and sulfate, the exact composition varying with the composition of the underlying grain surface. Outside this gelatinous layer, small rods of AFt can already be seen after as little as 10 minutes hydration (Fig. 5) and after about one hour these rods can be clearly seen on dried fracture surfaces (Fig. 6).<sup>6,15,30,32,33</sup> In the environmental cell they can be observed dispersed on the carbon support film at some distance from the surface of the hydrating grain,<sup>30</sup> indicating that they form by a through-solution mechanism. When cement paste is dried, the gelatinous layer collapses and shrinks back on to the surface of the grains. It is difficult to identify this product on fracture surfaces, although indications of some gelatinous product can be seen in ion-beamed thinned sections (Fig. 7).<sup>6,30</sup> The AFt rods also fall back onto the surface of the grains, although the density of rods is probably still related to the composition of the underlying grain. After some three hours hydration, the amount of C-S-H formed is sufficient for this phase to be identified on fracture surfaces as small spiky outcrops on the surface of the grains (Fig. 8).<sup>6,33,34</sup>

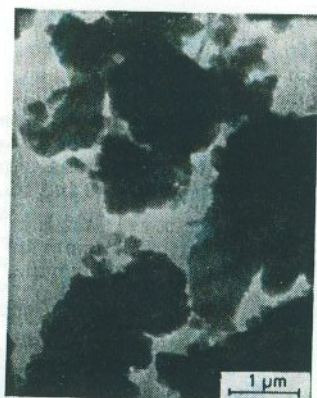


Fig. 5. (Left) Cement paste hydrated for 10 min\* in the environmental cell of the HVEM. The surfaces of the grains have a gelatinous appearance and several short rods of AFt can also be seen.

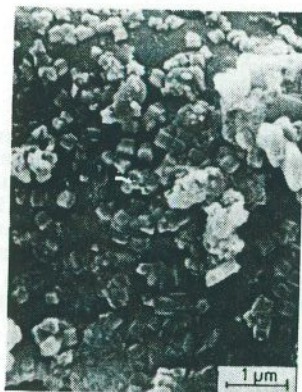


Fig. 6. (Right) Dried fracture surface in the SEM of cement paste hydrated for 1 h. Many rods of AFt can be seen.



Fig. 7. (Left) Ion-beamed thinned section of cement paste hydrated for 2 h (STEM). Product with a gelatinous appearance can be seen with some AFt rods.

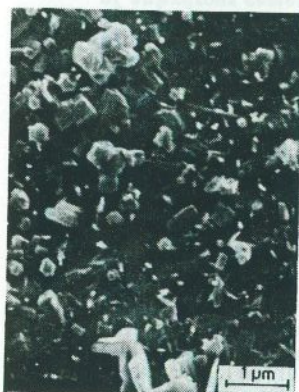


Fig. 8. (Right) Fracture surface of 3-h-old paste. Spiky outcrops of dried C-S-H can be seen among the AFt rods.

\*The w/c ratio of all the pastes illustrated is 0.5 unless otherwise stated.



## II (3 to 24 Hours)

The end of the induction period is marked by the rapid growth of both C-S-H and CH. In the undried state, C-S-H has a filmy, foil-like morphology, (Fig. 9), which dries to a fibrillar morphology (diamond type I) where there is plenty of space, and to a honeycomb morphology (diamond type II) where space is more restricted. (The presence of foreign ions such as  $\text{Cl}^-$  may also affect the morphology of C-S-H.) Small grains of cement (which probably contain only alite) hydrate rapidly to give rosettes or spherulites of C-S-H (Fig. 10).

In ion-beam thinned sections (Fig. 11), it can be seen that the C-S-H shell is separated from the underlying grain. This separation can be observed after as little as five hours hydration<sup>6,15</sup> and is thought to occur because the C-S-H nucleates outside the gelatinous layer formed earlier, on a framework of Aft rods. The space which is observed in dried sections is most likely filled with a highly concentrated or possibly colloidal solution in the wet state, although the discontinuity between the hydrate shell and core can also be seen in undried samples examined in the environmental cell (Fig. 12).<sup>6</sup> The growth of C-S-H between the cement grains bonds the paste together, causing the paste to set after about 3 to 4 hours of hydration. After about 12 to 18 hours, this bonding is strong enough for fracture to occur through the hydrate shells, such that the separation between them and the anhydrous core can be seen on fracture surfaces (Fig. 13). Such separated shells, which are completely hollow in some cases, were first noted by Hadley<sup>34</sup> on fracture surfaces

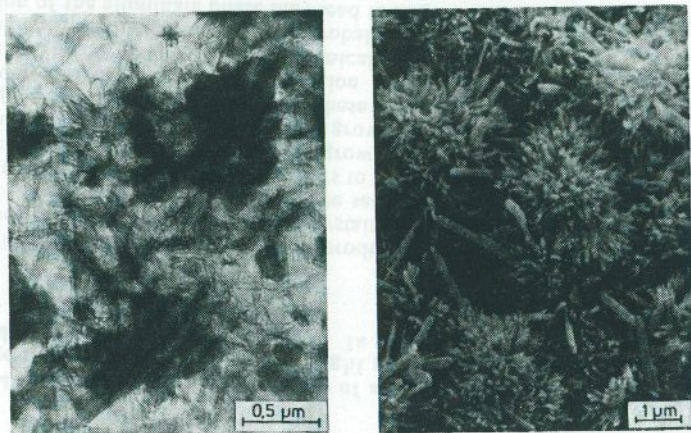


**Fig. 9. (Left) One-day-old paste in the environmental cell of the HVEM. The C-S-H which formed through solution during the major heat evolution peak has a morphology of crumpled foils; some rods of Aft can also be seen.**

**Fig. 10. (Right) Fracture surface of one-day-old paste in the SEM. 'Rosettes' of dried fibrillar C-S-H (diamond Type I) and long rods of Aft from the secondary reaction of the aluminat phase can be seen.**



**Fig. 11.** Ion-beam thinned section of a 12-h-old paste (STEM). Shells of hydration product can be seen around, but separated from, the dark anhydrous cores. Rosettes from the hydration of small grains and some hollow shells of C-S-H can also be seen.



**Fig. 12.** Undried, one-day-old paste (environmental cell, HVEM). Although this is not a cross-section, there is a region of low-density material visible between the hydrate shell and core.

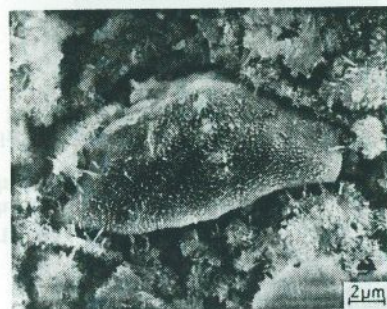


**Fig. 13.** Partially reacted grain of anhydrous cement with a separated shell of hydration product revealed on the fracture surface of a one-day-old paste. Rods of AFt and plates of AFm can be seen between the shell and core.

and such phenomena are often referred to as "Hadley grains." During fracture, large anhydrous cores may fall out, to leave large hollow shells. However, on polished sections, while it can be seen that practically all grains have separated hydrate shells (Fig. 14), the separation between shell and core is seldom more than about 1 μm.

The separation between the reacting grain and the C-S-H product indicates that the formation of the latter occurs by a through-solution mechanism. At this stage the shell is very open and porous and ions migrate through it, leading to the growth of C-S-H on the outer surface of the shell and increasing the separation between shell and core.

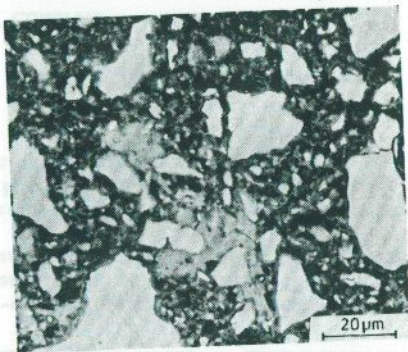


**Fig. 14.** Backscattered electron image of a polished section of a 12-h-old paste. A large mass of calcium hydroxide (light gray) can be seen. This has grown around many of the hydrating grains. In this paste almost all of the cement grains have separated hydrate shells.

The calcium hydroxide which is produced by the reaction of the silicate phases is deposited as massive hexagonal crystals in the space originally occupied by the water. In bse images this phase can be seen as extensive light-gray areas (Fig. 14). The number of nucleation sites appears to be small and the crystals may engulf some of the smaller cement grains as they grow.

After about 16 hours, a renewed growth of AFt occurs with long rods growing through the C-S-H layer (Fig. 10). These microstructural changes correspond to the shoulder on the main heat evolution peak which is sometimes observed in calorimetric curves.<sup>6,27,35</sup> The chemical changes responsible for this secondary reaction of the aluminate phase are probably related to the reaction of the alite. This reaction of the aluminate phase may lead to larger local separations between the core and its hydrate shell.

At the end of the main heat evolution peak, all grains smaller than about  $5 \mu\text{m}$  will have completely hydrated. Many of these which originally contained some aluminate phase will leave hollow shells of hydration product.

### III (24 Hours Onward)

As the hydrate shell thickens, it becomes less permeable and continuing reaction of alite leads to deposition of C-S-H on the inside of the shell. As the volume of C-S-H formed is greater than that of the alite which reacts, this process decreases the separation between shell and core. If the grains are large enough, this separation disappears after about seven days hydration, by which time the shell is about  $8 \mu\text{m}$  thick (Fig. 15). Further hydration of alite is very slow, with change being observable only on the scale of years. There is evidence to suggest that this period of hydration occurs by a topochemical mechanism, as suggested by Taylor.<sup>36</sup> In old pastes, three regions of C-S-H product can be identified in the relics of fully hydrated grains (Fig. 16).<sup>37</sup> The outermost of these is a thin layer ( $\approx 1 \mu\text{m}$ ) of "outer" C-S-H which formed through solution, in the originally water-filled space, during the major heat evolution peak. Inside this is a layer, about  $8 \mu\text{m}$  thick, which formed through solution while

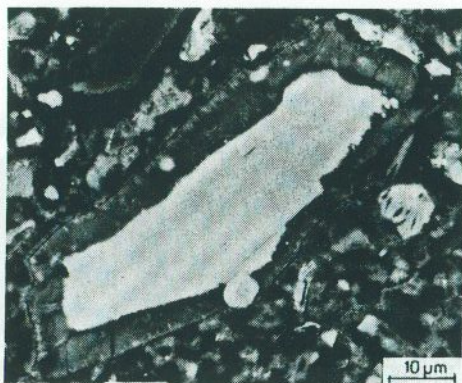


**Fig. 15.** Partially hydrated grain in a 69-day-old paste (bse image of polished section). At the outer edge of the hydrate shell a thin layer of 'outer' C-S-H formed during the main heat evolution peak can be seen. Inside this is a layer of C-S-H formed through solution infilling the separation between shell and core. Within this layer, along the bottom edge of the grain, is a rounded crystal of unreacted belite. At the top right edge is a region of unreacted ferrite. (Courtesy of K. D. Baldie.)

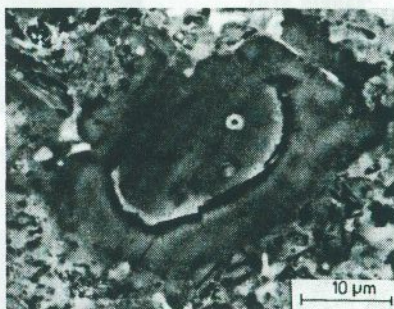


**Fig. 16.** Relic of fully reacted grain in a 23-year-old paste (bse image). In addition to the two regions of C-S-H identified in Fig. 15, there is an inner region formed by a topochemical mechanism.

the hydrate shell was separated from the anhydrous core. This is almost all "inner" product, occupying space originally filled by the anhydrous grain. The innermost region is also "inner" product, in this case formed by a topochemical or solid state mechanism.



Fig. 17. Fracture surface of a 14-day-old paste. The edge of a hydrate shell runs diagonally across the micrograph. On the inner surface (top left) many plates of AFm can be seen. Outside the shell AFt rods protrude into the pore space. (Courtesy A. Ghose.)

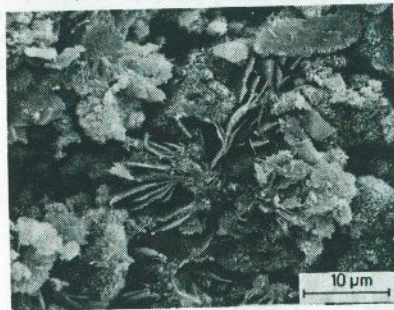
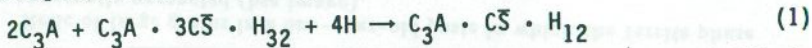


Fig. 18. Fracture surface of a one-day-old white cement (63% alite, 27% belite, 5% aluminate by QXDA). The aluminate phase, unrestricted by ferrite, has led to the formation of large AFm plates.

Inside the shell, the concentration of sulfate in solution drops rapidly as the aluminate phase reacts. This results in the reaction of further aluminate phase with any AFt present on the inside of the shell to give AFm according to the reaction (ignoring any substitution of iron):



The heat produced by this reaction is sometimes visible as a low, broad peak in the rate of heat evolution, as noted by Pratt and Ghose.<sup>35</sup> The direct conversion of AFt to AFm in the absence of aluminate phase does not appear to occur in cement. On fracture surfaces, AFm may be observed inside the hydration shells and AFt outside in the same specimen (Fig. 17).<sup>6,30</sup> However, if the concentration of sulfate ions in solution drops before the hydrate shells have thickened and partially isolated the anhydrous grains, much larger plates of AFm may be formed throughout the paste, as has been observed in some white cements which contain no ferrite phase (Fig. 18).<sup>6</sup>

The belite phase appears to take little part in the early hydration reaction. Small regions of belite within alite may be left unreacted (Fig. 15). After about 14 days,

the surfaces of belite particles revealed on fracture surfaces show signs of local reaction (Fig. 19),<sup>35</sup> although there is still relatively little hydration product visible around the particle after several months (Fig. 20). This reaction appears to occur preferentially along the twin boundaries. In a 23-year-old paste, the belite grains have completely hydrated, although the original lamellar of the twin structure is preserved (Fig. 21).<sup>37</sup> This strongly suggests that hydration has occurred topochemically, as originally suggested by Funk<sup>38</sup> and McConnell.<sup>39</sup>

The ferrite phase appears virtually unreacted in bse images of polished surfaces (Fig. 22), even in pastes many years old. Close examination of a 23-year-old paste<sup>37</sup>

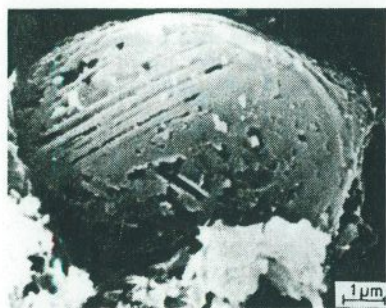


**Fig. 19.** Belite crystal revealed on the fracture surface of a 14-day-old paste, showing signs of local reaction. (Courtesy A. Ghose.)

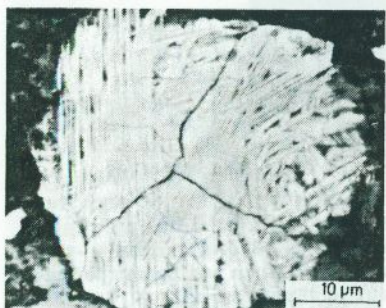


**Fig. 20.** Backscattered electron image of belite crystal in a 3-month-old paste showing preferential reaction along the twin planes.

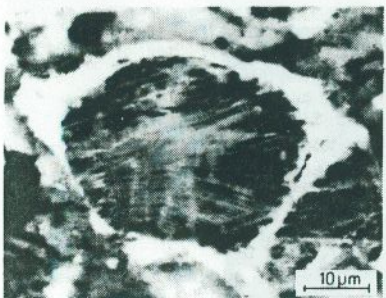


**Fig. 21.** Relic of fully reacted belite crystal in 23-year-old paste. The original twin lamellas can still be identified (bse image).

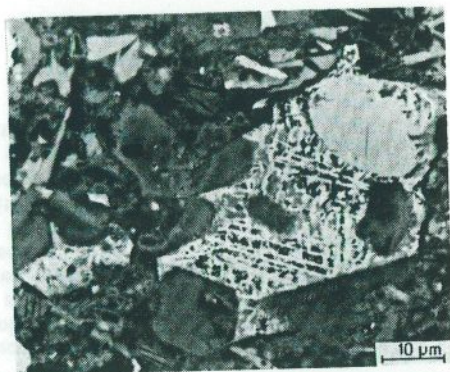


Fig. 22. Relic of large grains in a one-year-old paste in which the ferrite phase (white) is apparently unreacted (bse image).

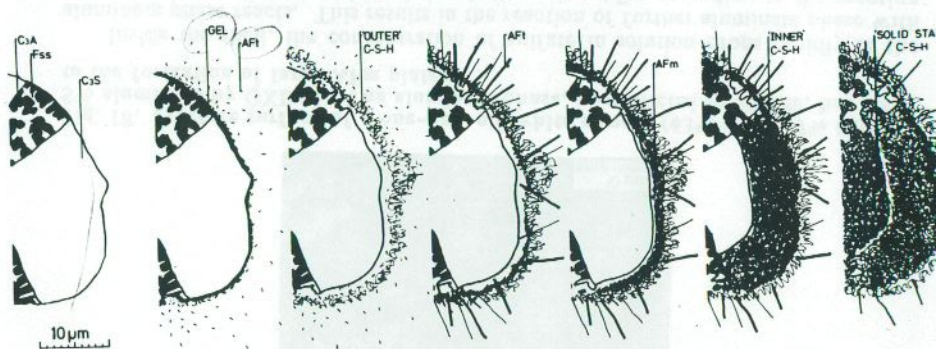
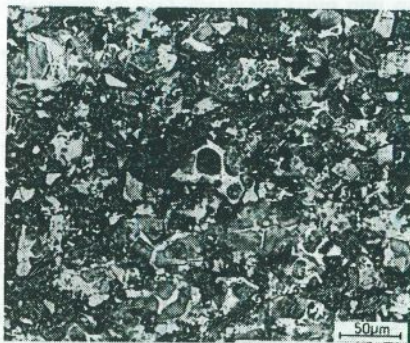


Fig. 23. Summary of microstructural development for a grain of cement. (a) Unhydrated section of polymineralic grain (scale of interstitial phase is slightly exaggerated). (b) -10 min. Some  $C_3A$  (and/or  $Fss$ ) reacts with calcium sulfate in solution. Amorphous, aluminate-rich gel forms on the surface and short  $AFt$  rods nucleate at edge of gell and in solution. (c) -10 h. Reaction of  $C_3S$  to produce "outer" product  $C-S-H$  on  $AFt$  rod network leaving  $\sim 1 \mu m$  between grain surface and hydrated shell. (d) -18 h. Secondary hydration of  $C_3A$  (and/or  $Fss$ ) producing long rods of  $AFt$ .  $C-S-H$  inner product starts to form on inside of shell from continuing hydration of  $C_3S$ . (e) 1-3 days.  $C_3A$  reacts with any  $AFt$  inside shell forming hexagonal plates of  $AFm$ . Continuing formation of "inner" product reduces separation of anhydrous grain and hydrated shell. (f) -14 days. Sufficient "inner"  $C-S-H$  has formed to fill in the space between grain and shell. The "outer"  $C-S-H$  has become more fibrous. (g) -years. The remaining anhydrous material reacts by a slow solid state mechanism, to form additional "inner" product  $C-S-H$ . The ferrite phase appears to remain unreacted.

has revealed two distinct regions in the iron-rich areas. It is possible that there is some leaching of calcium and aluminum from the outer layer to leave amorphous, hydrous ferric oxide. If the interstitial phases are intimately mixed, the reaction of aluminate phase will probably be restricted.

The development of microstructure for a large grain of cement is summarized in Fig. 23. After the first day or so, the net movement of ions during the hydration process is very small. This fact was noted by Taylor and Newbury<sup>40</sup> from their electron microprobe study of a cement paste which had been cured for 23 years. In bse images of this (Fig. 24) and other mature pastes, the relics of original cement grains can be identified. Nevertheless, the continued growth of calcium hydroxide and some C-S-H in the originally water-filled space has gradually reduced the volume and connectivity of the large pores.



**Fig. 24.** Microstructure of a 23-year-old paste (bse image). This paste is fully reacted apart from the bright regions of ferrite phase; these help to identify the relics of the original grains which now mainly consist of dense 'inner' C-S-H. Among the relics can be seen tortuous regions of calcium hydroxide and a mixture of other hydration products (dark gray) and porosity (black).

### Effect of Mineral Replacements on Microstructure

Various minerals are often used in concrete as partial replacement for cement. These minerals have some capacity to hydrate, usually reacting with calcium hydroxide, to give space-filling product and thus refining the porosity of the paste. The most widely used mineral replacements are fly ash, blast-furnace slag, and silica fume. The fly ash is generally used at replacement levels of up to about 30%. For slag replacements, levels at around 40% and around 70% are used for different applications. With these two minerals the development of microstructure of the paste during hydration is only slightly modified from the pattern previously described. The replacement levels for silica fume are much lower, typically around 10%, but the effects on the microstructural development are much more dramatic.

Fly ash is a by-product of coal burning in power stations and consists of small spherical particles with a similar particle-size distribution to anhydrous cement. About 80% of a fly ash is a reactive silica glass containing calcium, aluminum, iron, and other minor oxides. The crystalline content is typically mullite, ferrite, and quartz. In cement paste, the glassy component of the fly ash undergoes a pozzolanic reaction with the calcium hydroxide produced by the cement to give C-S-H.



In terms of microstructural development, fly ash starts to react only after several days hydration, although impurities, such as alkali sulfates, in the fly ash may affect the hydration of the cement earlier. Nevertheless, deposition of C-S-H and Aft from the reaction of the cement may be observed on the surface of the fly ash particles, almost immediately in the environmental cell (Fig. 25)<sup>41</sup> and after several hours on fracture surfaces.<sup>42,43</sup> After several days the dissolution of the glassy phase can be seen on fracture surfaces, where the crystalline material in some of the larger particles has been exposed (Fig. 26).<sup>44</sup> Rims of hydration product can also be seen around the fly ash particles on fracture surfaces and in bse images of polished sections (Fig. 27).



**Fig. 25.** Cement/fly ash paste (70/30), hydrated for 10 min (TEM environmental cell). Product can be seen on the cement grains and deposited on the surfaces of the spherical fly ash particles.

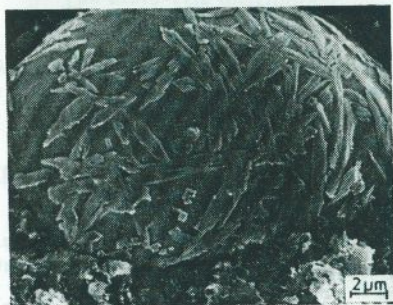


**Fig. 26.** Large particle of fly ash on the fracture surface of a 28-day cement/fly ash paste. Reaction of the glassy phase in the fly ash has exposed some crystalline material. (Courtesy of Y. Halse.)

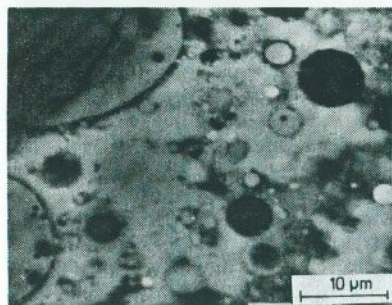


**Fig. 27.** Backscattered electron image of a 69-day-old cement/fly ash paste. Several particles of fly ash are visible in a massive region of calcium hydroxide, some of which show signs of reaction.

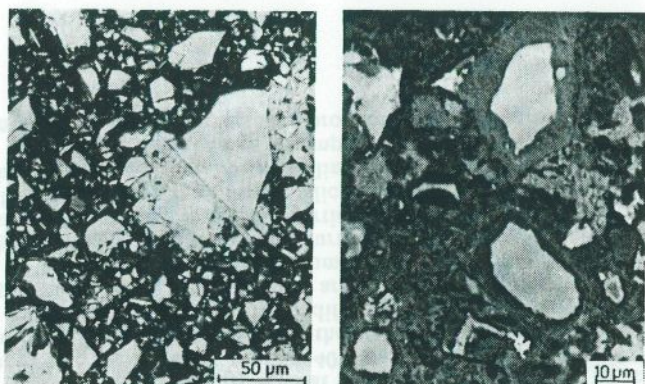


**Fig. 28. (Left)** Backscattered electron image of cement/slag paste (30/70) hydrated for one day. A large mass of calcium hydroxide has grown around a collection of angular slag grains. (Courtesy of M. P. Cook.)

**Fig. 29. (Right)** Partially hydrated cement grain (top) and slag grain (bottom) in an 8-month-old cement/slag paste (60/40). The different gray level of the hydration rims indicates their different composition (bse image).

Blast-furnace slags have a glass content of about 90% glass of typical composition: 35%  $\text{SiO}_2$ , 45%  $\text{CaO}$ , 10%  $\text{Al}_2\text{O}_3$ , 8%  $\text{MgO}$ , and small amounts of other oxides. Although slags have some inherent hydraulicity, an activator (such as calcium hydroxide) is needed and the slag plays little active part in the early microstructural development. However, it does appear to have some effect on the distribution of calcium hydroxide. In bse images of slag/cement pastes (Fig. 28), it is noticeable that large masses of CH have grown around the slag particles. Over a period of several months the slag slowly reacts and the amount of calcium hydroxide decreases. In old pastes, reaction rims can be seen around the slag particles (Fig. 29); these are darker (with a lower average atomic number) than the hydration product around the cement grains and contain significant quantities of  $\text{MgO}$ . Such layers have also been noted by Tanaka et al.<sup>45</sup> Analytical work by Harrison et al.<sup>46</sup> suggests that these rims are composed of C-S-H mixed on an atomic scale with another product, possibly a hydrated magnesium aluminate of the hydrotalcite group.

Silica fume consists of very small particles ( $\approx 0.1 \mu\text{m}$ ) of amorphous silica. The high surface area of the fume means that it reacts much more rapidly than fly ash or slag. As it is very difficult to disperse the silica fume, superplasticizers are always added to such mixes in practice. Several workers have noted that the microstructure of pastes containing silica fume is very different from that developed in ordinary cement pastes,<sup>47,48</sup> having a dense amorphous appearance. The bse image of a mature cement silica fume paste (Fig. 30)<sup>49</sup> illustrates this dense microstructure. Despite the use of superplasticizer, some clumps of fume are still present (these are marked Si in the micrograph). Some large cement grains appear to have hydrated to leave hollow pores containing unreacted ferrite phase. The reasons for these differences in microstructural development are not fully understood at present. Silica fume also appears to have a profound influence on the microstructure of the interface between cement past and aggregate, which will be discussed subsequently.

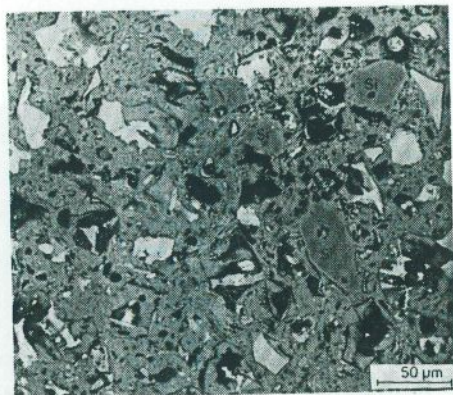


**Fig. 30. Polished section of a mature cement/silica fume paste (85/15). Clumps of silica fume can be identified (Si). No massive regions of calcium hydroxide can be seen. Some of the large pores are associated with the hydration of cement grains to leave hollow shells of hydration product.**

### Characterization of the Overall Paste Microstructure

In the previous sections the development of microstructure was described mainly in terms of the local changes which occur around individual grains of cement during hydration. The resulting microstructure for a given paste will depend on:

1. The phases present and their distribution within the grains.
2. The grain-size distribution.
3. The amount of reaction (related to age, moisture state, and temperature).
4. The water/cement ratio.

The first two are determined by the anhydrous cement powder, whose characterization has already been discussed. The grain size, in conjunction with the degree of reaction, is particularly important in determining the distribution of the C-S-H product in the microstructure. As previously indicated, grains smaller than about  $5\ \mu\text{m}$  (about 6 wt% of the total) will hydrate completely during the major heat evolution peak to give "outer" C-S-H in the originally water-filled space. Grains between about 5 and  $15\ \mu\text{m}$  (about 30 wt%) will have reacted after about seven days to give "outer" and "through solution, inner" C-S-H. Only the cores of grains larger than about  $15\ \mu\text{m}$  will then eventually hydrate to give "solid state, inner" C-S-H.

The water/cement ratio determines the amount of water-filled space in the fresh cement pastes; for a w/c of 0.5 this is about 60%. At early ages the effect of the w/c ratio on the appearance of fracture surfaces is quite dramatic (Figs. 31 and 32). After 18 hours, the fracture of the cement paste with w/c = 0.5 is almost completely interparticular (Fig. 31), whereas, in the paste with w/c = 0.3, the closer spacing of the cement grains means that more bonding has occurred and there is more fracture through the shells, revealing more anhydrous cores on the fracture surface (Fig. 32). At later ages the effect of w/c ratio on the microstructure is less obvious.

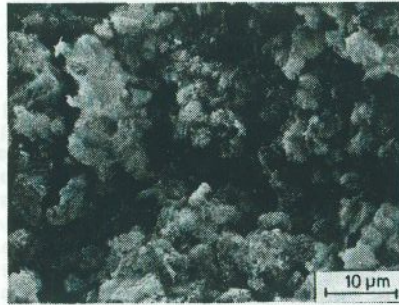


**Fig. 31. Fracture surface of cement paste with  $w/c = 0.5$ , hydrated for 18 h. The fracture has been predominantly interparticular.**

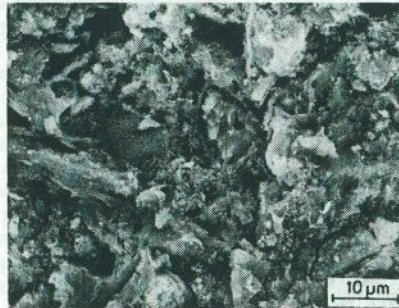


**Fig. 32. Fracture surface of cement paste with  $w/c = 0.3$ , hydrated for 18 h. In this case there has been more fracture through the hydrate shells, revealing the separation between these shells and the anhydrous cores.**

Given these various factors, quantitative descriptions are necessary for microstructural characterization. The simplest means of quantification is to determine the relative proportions of the constituents present. The gray-level contrast between the microstructural constituents in bse images makes it possible for them to be discriminated by an automatic image analyzer, as illustrated in Fig. 33. This method can be used to measure the quantities of anhydrous material, massive calcium hydroxide, other hydration products, and pores. If a sufficiently large area is analyzed, the quantities determined will be representative of the bulk paste. Although the same quantities can be measured by indirect techniques, several techniques must be used to measure all the constituents. A study by Scrivener et al.<sup>22</sup> showed that measurement of the amount of unreacted anhydrous material by analysis of bse images gives comparable results to values measured by loss on ignition (Fig. 33(f)). The measurements of porosity by the image analysis method were lower than those obtained by methanol replacement, owing to the limited resolution ( $0.5 \mu\text{m}$ ) of

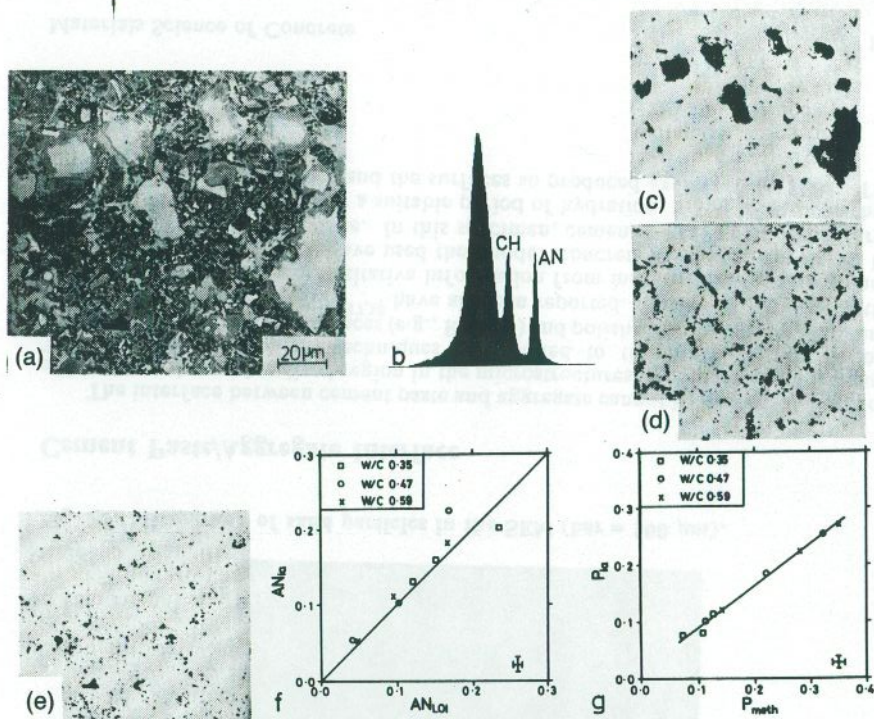


**Fig. 33.** Analysis of microstructural constituents in cement paste. (a) Bse image from 28-day-paste; (b) gray-level histogram, showing peaks for: anhydrous material (AN), calcium hydroxide (CH), and other hydration products; (c) anhydrous material; (d) calcium hydroxide; (e) porosity; (f) comparison of anhydrous material measured by image analysis (ia) and by loss on ignition (LOI); (g) comparison of porosity from image analysis and methanol absorption.

the bse images at the magnification used ( $\times 400$ ). Nevertheless, there was good proportionality between the two sets of measurements for pastes at a wide range of ages and w/c ratios (Fig. 33(g)). It should also be possible to determine the amount of calcium hydroxide by this method, but, because of the uneven distribution of this phase, measurements must be made over a larger area than was done in this study.

The importance of the analysis of bse images lies in the potential it offers for obtaining quantitative descriptions of the distributions of the microstructural constituents. The choice of suitable parameters to characterize a distribution must be considered carefully and the best strategy will depend on the nature of the distribution and the end purpose of the characterization. It is also important to understand the stereological problems involved in trying to derive information about three-dimensional distributions from the study of two-dimensional sections.

The anhydrous material exists as discrete particles. In this case the distribution of particle sizes might be suitable for some applications, while for others the total

surface area of the grains or the uniformity of their distribution in space might be a more appropriate description of the microstructure.

In contrast, the pores in cement paste are not discrete and the connectivity of the pore space has an important influence on such properties as permeability. In this case the pore-size distribution and connectivity measured in two-dimensional sections may bear little or no relation to the three-dimensional pore structure. For some purposes, characterization of the pore surface may be more appropriate and here concepts such as fractals may be important.<sup>50,51</sup>

The distribution of calcium hydroxide poses similar problems due to the tortuous shape of the crystalline masses. Here the density of nucleation sites might be an important parameter, which could be estimated by analysis of nearest-neighbor distances.

It is clear that there is much to be done in this area, but with appropriate basic work it should be possible to establish ways of characterizing the microstructure of cement paste, which will further the understanding of its behavior.

## Aggregates

A very wide range of aggregates is used in the production of concrete. Empirically, several factors have been established as affecting the workability of the fresh concrete and the durability of the hardened structure.<sup>52</sup> These factors may be summarized as follows:

*Physical characteristics of the aggregate particles:* the particle-size distribution (grading); the particle shape; the surface texture of the particles.

*Impurities and contaminants:* Clay, silt, and dust; organic matter; mica, chalk, shell; sulfates and chlorides; metallic impurities, in particular lead and zinc oxides.

*Mechanical and chemical stability:* mechanical strength; susceptibility to reaction with alkalis; soundness with respect to freezing and thawing.

During the early stages of hydration, the aggregate does not play an active role in microstructural development. Thus, in the absence of significant amounts of impurities or contaminants, the physical properties of the aggregate are of most importance. In particular, the grading of the aggregate will affect the packing of the particles in the concrete and the surface area of aggregate which must be covered by cement paste. It is difficult to characterize features such as particle shape and texture in a quantitative manner; in particular, a surface may be described as rough on several different scales.

Examples of two commonly used aggregates are shown in Figs. 34(a) and (b). The aggregate in Fig. 34(a) is a natural gravel aggregate; the particles are generally rounded and have a wide range of surface textures. The other aggregate is a crushed granite rock. In this case the particles are angular and the surface is fairly uniform. The speckled appearance indicates the polymineralic nature of this aggregate. Figure 35 shows the surface of a fine aggregate sand taken by SEM; some particles are fairly smooth, while others are pitted.

Over periods of several years, some aggregates may undergo chemical reaction. The most serious of these reactions is the aggregate alkali reaction (AAR), in which components of the aggregate react with alkalis in the cement paste to give a gel, which may imbibe water and swell, causing cracking in the concrete. The AAR is most commonly caused by the presence of amorphous or microcrystalline silica in the aggregate, but has also been reported with carbonate aggregates.

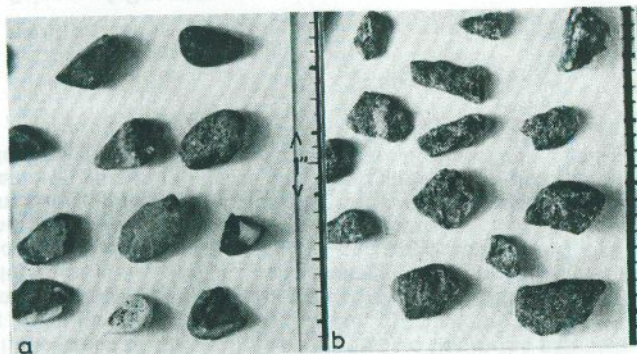


Fig. 34. Photographs of (a) gravel and (b) crushed granite. (Courtesy of A. K. Crumble.)

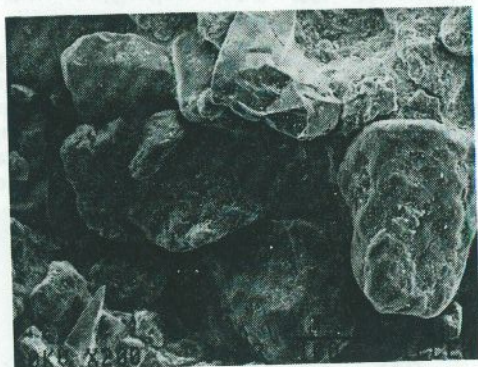
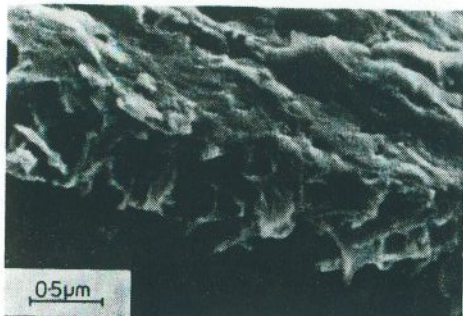


Fig. 35. Micrograph of sand particles in the SEM (bar = 100  $\mu\text{m}$ ).

### Cement Paste/Aggregate Interface

The interface between cement paste and aggregate cannot be studied in isolation as it exists only as a localized region in the microstructures of concretes and mortars. This makes microscopical techniques well suited to the study of this region. Examinations of fracture surfaces (e.g., Ref. 53) and polished surfaces<sup>54</sup> by SEM, and ion-thinned sections by TEM<sup>17,18</sup> have all been reported. However, because of the difficulties in obtaining quantitative information from microscopical studies, many workers (e.g., Refs. 55-60) have used the "model" concrete specimen, developed by Farran<sup>61</sup> to study the interface. In this specimen, cement paste is cast onto a large flat piece of aggregate. After a suitable period of hydration, the specimen can then be fractured at the interface and the surfaces so produced examined by SEM. The



**Fig. 36.** Layer of product deposited on aggregate surface in four-day-old mortar.

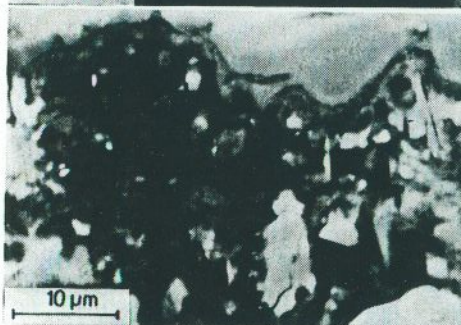


**Fig. 37.** Microstructure at edge of sand grain in one-day-old mortar. There is a layer of C-S-H product along the surface of aggregate.



**Fig. 38.** Contact zone between calcite and cement paste, ion-beam-thinned section of a one-year-old sample. (Courtesy J-P Ollivier.)



**Fig. 39.** Area of fracture surface in a one-day-old mortar, adjacent to an aggregate particle. Beyond the surface layer (some of which adhered to the aggregate during fracture) can be seen 'rosettes' of C-S-H from the hydration of small cement grains and long rods of Aft.



concentration and orientation of phases in the interfacial region can also be analyzed by the technique developed by Grandet and Ollivier,<sup>55-57</sup> which involves successive abrasion of the cement paste side of the interface and examination of the phases present on the surface by X-ray diffraction. This type of specimen also facilitates microstructural examination by SEM, when it is fractured along the interface. As a model for concrete there are several disadvantages to this specimen configuration. First, the surface of the aggregate is flat and often polished; second, the aggregate is not present during the mixing process, and third, there is a considerable thickness of paste in contact with the aggregate as opposed to the narrow bands of paste between aggregate particles in concrete.

Microstructural studies indicate that a thin layer of hydration product ( $\approx 1 \mu\text{m}$  thick) forms on the surface of the aggregate. From their studies of cement paste cast against glass slides,<sup>62</sup> Barnes et al. suggested that this is a duplex layer with a thin film of calcium hydroxide adjacent to the aggregate surface surrounded by a layer of C-S-H. However, Scrivener and Pratt<sup>64</sup> found no evidence of the calcium hydroxide film in their study of mortars examined as fracture surfaces (Fig. 36) and as polished sections with bse (Fig. 37). Even with the higher resolution possible with transmission electron microscopy, there appears to be only a simple layer of product in contact with the aggregate in the work of Javels et al.<sup>17,18</sup> (See Fig. 38.) The deposition of this product layer does not entail any chemical reaction with the aggregate, which merely acts as a nucleation site. However, at later ages there may be a chemical reaction between this layer and some carbonate aggregates, producing a stronger bond.<sup>18,63</sup>

Beyond this layer of product there is a region of high porosity which is known as the "aureole de transition." This arises because the large anhydrous cement grains cannot pack close to the aggregate particles. In composite specimens this region is characterized by the preferred orientation of calcium hydroxide with the *c* axis parallel to the aggregate surface, and by increased concentrations of AFt<sup>55-58</sup> which extend some  $50 \mu\text{m}$  into the cement paste. On fracture surfaces of concretes and mortars, this region can be seen through openings in the surface layer where it is incomplete or has remained attached to the aggregate particle (Fig. 39). In this region there are many "rosettes" of C-S-H from the hydration of small grains and a large number of long AFt rods. In bse images of polished sections, the distribution of cement grains can be observed directly or deduced from relics in mature specimens. Figure 40 shows the interfacial region in a one-day-old mortar. There are few large grains close to the interface and, in this case, there appears to be a concentration of small grains in the crevices of the aggregate particles, which probably accumulated as the mortar was mixed. The numerous small grains close to the interface lead to many hollow hydration shells being observed in this interfacial region which can still be seen in mature specimens (Fig. 41). It is perhaps no coincidence that Hadley first observed hollow hydration shells (Hadley grains) while studying interfacial regions in concrete.<sup>34</sup> As discussed earlier, there tends to be a higher proportion of interstitial phases exposed on the surfaces of smaller grains, which would account for the high concentration of AFt observed in this region. In bse images, crystals of calcium hydroxide can be seen in the interfacial region (e.g., Fig. 40), but it is difficult to identify any preferred orientation.

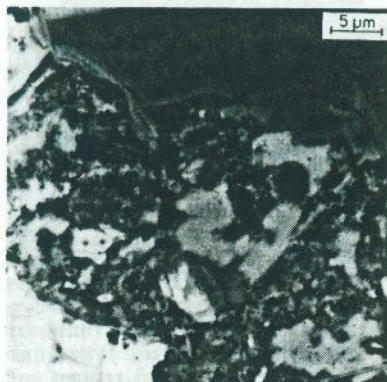
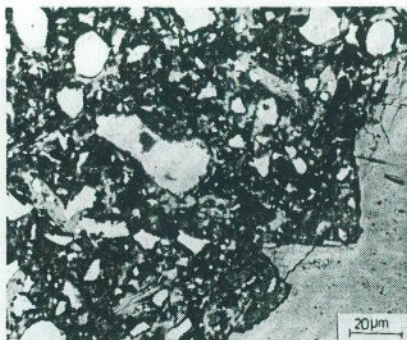


**Fig. 40. (Left)** Backscattered electron image of interfacial zone of a one-day-old mortar. There are few large cement grains close to the aggregate surface. There are many hollow shells of hydration product in the interfacial region. In the crevices of the aggregate surface, small grains of cement have accumulated during mixing, leading to more product in these regions. Several massive regions of calcium hydroxide (light gray) are also apparent with a range of orientations.

**Fig. 41. (Right)** High-magnification bse image of the interfacial region in a 10-week-old composite specimen (Ref. 65). Even in this mature paste, hollow shells of hydration product from the reaction of small grains can still be seen.

As the microstructural constituents can be distinguished in bse images of polished sections of concretes and mortars, this technique can be used to characterize the microstructure of the interfacial region quantitatively in real concretes and mortars. With an automatic image analyzer, the relative amounts of the constituents can be measured in bands spreading out from the aggregate surface, as illustrated in Fig. 42.<sup>64</sup> However, with random sections of concrete, the angle at which the aggregate surface intersects the plane of the section is unknown, and the normal distance from the aggregate surface to a point in the section can only be estimated.

In order to avoid this problem, Scrivener and Gartner<sup>65</sup> prepared specimens in which single pieces of aggregates were cast into blocks of cement paste. Sections were then cut from these specimens, normal to the aggregate surfaces. These sections were analyzed by the technique described above, averaging the results for each band over 10 fields covering about 200  $\mu\text{m}$  length of the aggregate surface. With this number of fields there was considerable scatter in the results, but there was a clear decrease in the amount of anhydrous material and increase in the porosity in an interfacial zone some 30 to 50  $\mu\text{m}$  deep (Fig. 43). A slight increase in the amount of calcium hydroxide close to the interface was also observed but this was not significant with regard to the scatter in the results. In terms of simulating concrete, these specimens have an advantage over composite specimens which use a flat piece of aggregate, by having an unprepared aggregate surface. However, the aggregate is still not present during mixing. The accumulation of small particles at the aggregate surface seen in Fig. 40 indicates that the movement of aggregate particles through the paste during mixing has an effect on the microstructure of the interfacial zone.

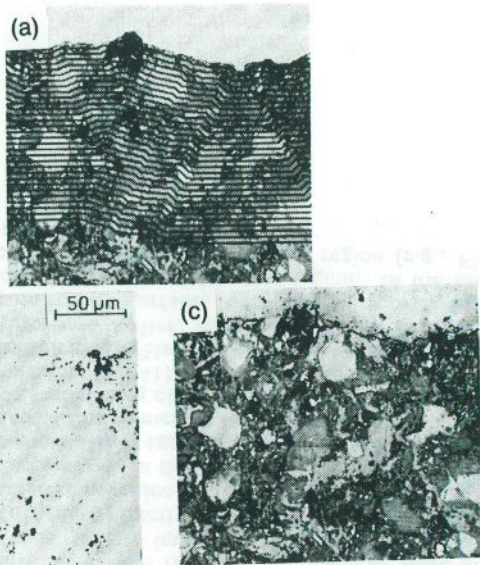


Fig. 42. Measurement of microstructural gradients in the interfacial region. (a) Bse image with aggregate particle at the top of the micrograph; (b) porosity detected in cement paste; (c) black lines indicate the bands in which the microstructural constituents are measured.

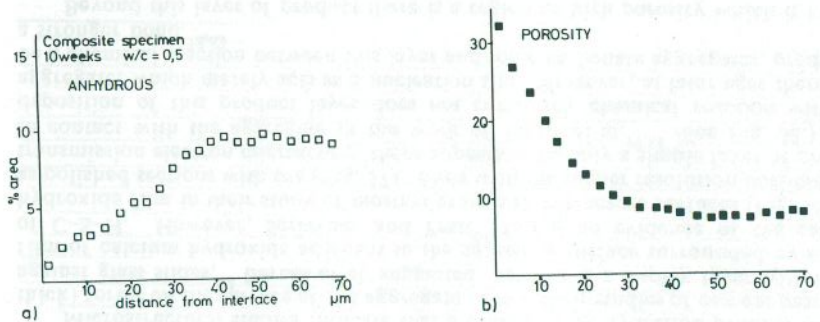


Fig. 43. Microstructural gradient in the interfacial region of 10-week-old composite specimens examined by Scrivener and Gartner (Ref. 65). The results plotted are the average measurements from 10 fields in each of three different aggregates. (a) Anhydrous material, (b) porosity.

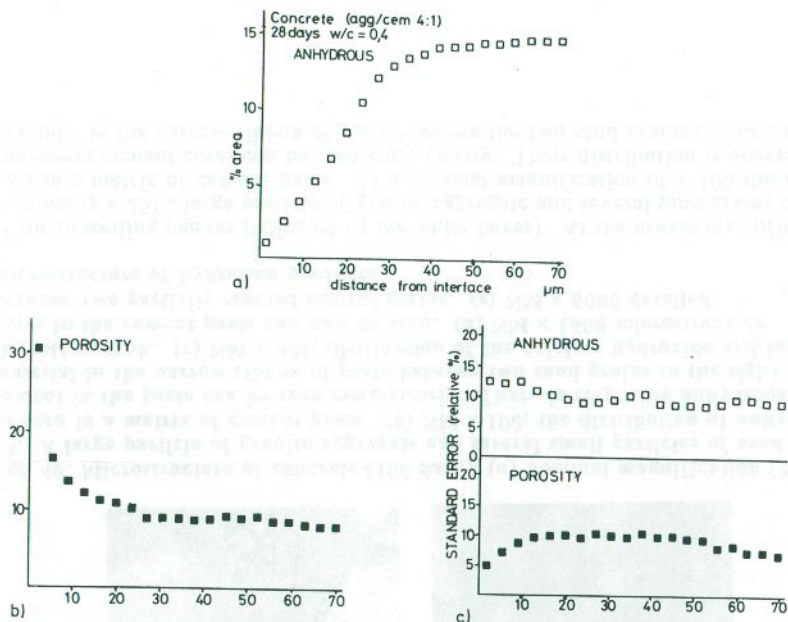


Fig. 44. Microstructural gradients in the interfacial region of 28-day-old concretes, average of 50 fields. (a) Anhydrous material, (b) porosity, (c) standard errors.

Despite the problem of the unknown angle of intersection of the aggregate with the plane of the section, it might be possible to apply this method to concrete if a large number of areas are analyzed. To investigate this possibility, Scrivener et al.<sup>66</sup> looked at the variability of the results when a large number of fields, selected in a "uniform random" manner, are analyzed. Some of the results from this work are shown in Fig. 44. In these graphs, the distances from the aggregate surface measured in the plane of the section have been estimated from the average angle of intersection of the aggregate surfaces with a random section. The proportions of the constituents change smoothly and the standard errors for the measurements are all around 10% of the measured values. From this preliminary study it appears that this method could be developed as a means of characterizing the interfacial zone in real concretes and used to investigate the effect that factors such as mix design or direction of casting have on this region.

All the quantitative studies, both on composite specimens and in concretes, indicate that the width of the interfacial zone is between 30 and 50  $\mu\text{m}$ . From Fig. 4 it can be seen that only about 15 to 20% of anhydrous grains are larger than 50  $\mu\text{m}$ . This seems to indicate that the essential feature determining the interfacial zone is the packing of the anhydrous cement grains against the "wall" of aggregate. However,

the type of specimen configuration, and especially the presence of the aggregate during mixing, may affect the gradients of microstructure in this zone.

### Effect of Silica Fume on the Interface

There is considerable interest in the incorporation of silica fume in mixes to produce high-strength concrete. This replacement material appears to have a profound effect on the microstructure of the interfacial region, consistent with the microstructure observed in silica fume/cement pastes. Figure 45 shows the microstructure of the interfacial zone in a concrete containing silica fume; the generally dense appearance of the microstructure is apparent. However fairly large pores are still present in the form of hollow hydrate shells. In contrast to the equivalent paste, the silica fume was well dispersed in the concrete, due to crushing or shearing between the aggregate particles, and no clumping of the silica fume was observed.<sup>49,65</sup> Scrivener and Bentur<sup>49</sup> analyzed microstructural gradients of the interfacial zones in high-strength concretes with and without silica fume. The gradient in the amount of anhydrous material was in both cases similar to that observed in the other studies described (Figs. 43(a) and 44(a)). This is consistent with the view that the particle-size distribution of the cement determines the width of the interfacial zone. The porosity gradient was much shallower in the concrete containing silica fume, as indicated by the appearance of the micrograph (Fig. 45); this suggests that the small particles of silica fume accumulate in the interfacial region during mixing.

### Overall Microstructure of Concrete

The microstructure of concrete is that of a composite material, composed of aggregate, cement paste, and the interface between them. The complexity behind this statement can be appreciated by observing the sequence of micrographs shown in Fig. 46, each of which was taken of the same area, at about four times the magnification

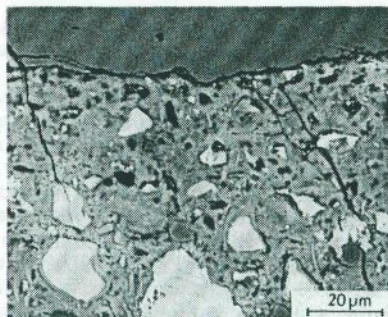


**Fig. 45.** Interfacial region of silica fume concrete. The microstructure is dense and there are no clumps of silica fume as seen in the cement/silica fume paste (Fig. 30). The hydration of some small cement grains has left some enclosed pores.

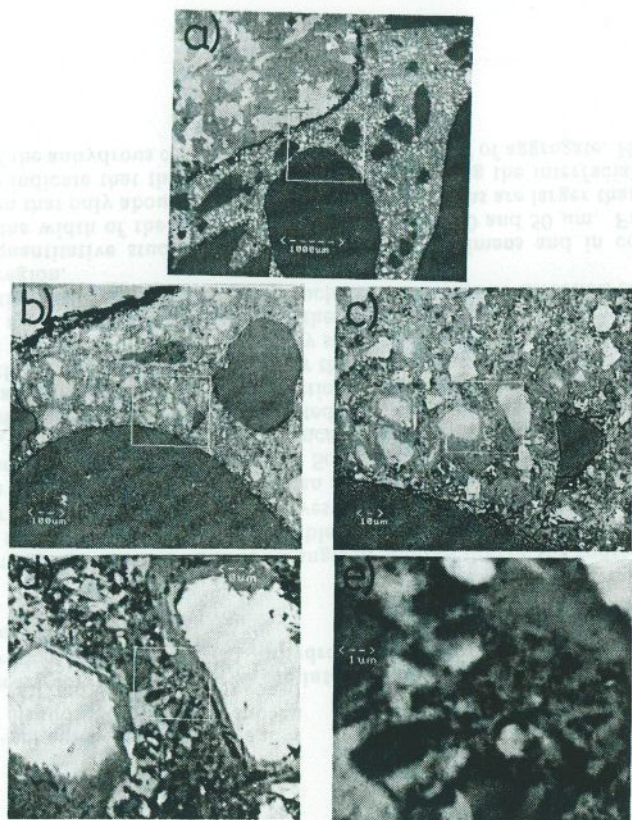


**Fig. 46. Microstructure of concrete (180 days): (a) nominal magnification (NM)  $\times$  25. A large particle of granite aggregate and several small particles of sand can be seen in a matrix of cement paste. (b) NM  $\times$  100; the distribution of anhydrous cement in the paste can be seen more clearly. There is very little anhydrous material in the narrow ribbon of paste between two sand grains to the right of the micrograph. (c) NM  $\times$  400; distribution of the calcium hydroxide and large pores in the cement paste can now be seen. (d) NM  $\times$  1600 microstructure between two partially reacted cement grains. (e) NM  $\times$  6000 detailed microstructure of hydration products.**

of the preceding one (as indicated by the white boxes). At the lowest magnification (nominally  $\times$  25) a large particle of granite aggregate and several sand grains can be seen in a matrix of cement paste. At a nominal magnification of  $\times$  100 the bright anhydrous cement cores can be seen more clearly. Their distribution is uneven; for example, in the narrow ribbon of paste between the two sand grains on the right of

the picture there is very little anhydrous material present. At  $\times 400$  the microstructure of the paste can be seen in more detail and the distribution of the larger pores can be seen. The next micrograph ( $\times 1600$ ) shows the microstructure between two hydrating cement grains and the final micrograph ( $\times 6000$ ) gives an impression of the morphology of the hydration products.

The characterization of the concrete microstructure entails the characterization of the cement paste and the paste/aggregate interface, which have already been discussed. In addition, the distribution of the aggregate particles and the incidence of features such as air voids and bleeding must be considered. In the case of real concrete structures, the microstructure may vary throughout the cast section. In particular it is essential to take account of the microstructure of the material near the surface, which plays a crucial role in protecting the reinforcing steel.

Kreijger<sup>67,68</sup> discussed the phenomenon of the concrete skin, which occurs whenever concrete is poured against a barrier or is leveled flat. This skin consists of an outer layer of cement paste some 0.1 to 0.3 mm thick, beneath which is a 3 to 5 mm thick layer of mortar. The water/cement ratio also varies in these surface layers. In addition, the gradients will also occur in the moisture state of this layer as water evaporates from the surface, as discussed by Parrott.<sup>69,70</sup> These effects will produce microstructural gradients extending some 50 mm into the concrete.

The fact that these phenomena produce variations of microstructure in space indicates that quantitative microscopy (both optical and with backscattered electrons) can play an important role in characterizing and understanding the surface region of concrete.

The microstructure of concrete continues to change throughout its life, due not only to continuing hydration but also to the effects of the environment. In particular, the ingress of other compounds such as carbon dioxide may have profound effects on the microstructure. The diffusion of such compounds will also produce gradients in the microstructure. In environments such as seawater, several different ionic species (e.g.,  $\text{Cl}^-$ ,  $\text{SO}_4^{2-}$ ,  $\text{Mg}^{2+}$ ) diffuse at different rates and the gradients they produce must be considered individually.

Despite these many complexities, "good" microstructural characterization of concrete is not an unrealistic goal. In qualitative terms, the way in which microstructure develops during the hydration of cement and concrete is fairly well understood. What are needed now are more quantitative descriptions of the microstructure, which can be related to its behavior. They will not necessarily entail complete quantification of every detail, but only by understanding the overall context can useful methods of characterization be established.

## Acknowledgments

The author would like to thank Dr. K. D. Baldie, Ms. M. P. Cook, Ms. A. K. Crumby, and Prof. P. L. Pratt for helpful discussions and the Warren Research Fund of the Royal Society for financial support.

## References

- <sup>1</sup>E. Hornbogen, "On the Microstructure of Alloys," *Acta Metall.*, **32**, 615-27 (1984).

- <sup>2</sup>H. F. W. Taylor, Chemistry of Cement Hydration; pp. 85-110 in Proceedings of the 8th International Congress on the Chemistry of Cement, Vol. I. Finep, Brazil, 1986.
- <sup>3</sup>H. F. W. Taylor, "Proposed Structure for C-S-H Gel," *J. Am. Ceram. Soc.*, 69 [6] 464-67 (1986).
- <sup>4</sup>S. Diamond, "Cement Paste Microstructure-An Overview at Several Levels"; pp. 2-30 in Hydraulic Cement Pastes: Their Structure and Properties. Cement & Concrete Association, Slough, U.K. 1976.
- <sup>5</sup>H. M. Jennings, "The Developing Microstructure in Portland Cement"; pp. 349-96 in Advances in Cement Technology. Edited by S. N. Ghosh. Pergamon, New York, 1983.
- <sup>6</sup>K. L. Scrivener, "The Development of Microstructure during the Hydration of Portland Cement; Ph.D. Thesis, University of London, 1984.
- <sup>7</sup>D. H. Campbell, Microscopical Examination and Interpretation of Portland Cement and Clinker. Portland Cement Association, Skokie, IL, 1986.
- <sup>8</sup>G. R. Long, "The Use and Application of Optical Microscopy in Portland Cement Clinker Research"; pp. 39-50 in Characterization and Performance Prediction of Cement and Concrete. Edited by J. F. Young. Engineering Foundation, New York, 1982.
- <sup>9</sup>E. Fundal, "Optical Microscopy of Cement Clinkers and Raw Mixes," FLS Review No. 25. F. L. Smidth, Copenhagen.
- <sup>10</sup>N. Thaulow, A. Damgaard Jensen, S. Chatterji, P. Christensen, and H. Gudmundsson, "Estimation of the Compressive Strength of Concrete Samples by Means of Fluorescence Microscopy," *Nordisk Betong*, 2-4, 51-52 (1982).
- <sup>11</sup>H. N. Walker and B. F. Marshall, "Methods and Equipment Used in Preparing and Examining Fluorescent Ultrathin Sections of Portland Cement Concrete," *Cem. Concr. Aggs.*, CACAGDP, 1, 3-9 (1979).
- <sup>12</sup>D. D. Double, "Some Studies of the Hydration of Portland Cement Using High Voltage (1 MeV) Electron Microscopy," *Mater. Sci. Eng.*, 12, 29-34 (1973).
- <sup>13</sup>D. D. Double, A. Hellawell and S. J. Perry, "The Hydration of Portland Cement," *Proc. R. Soc. (London), Sect. A.*, 359, 435-51 (1978).
- <sup>14</sup>H. M. Jennings and P. L. Pratt, "On the Reactions Leading to Calcium Silicate Hydrate, Calcium Hydroxide and Ettringite during the Hydration of Cement"; pp. II.141-II.146 in Proceedings of the 7th International Congress on the Chemistry of Cement, Vol. II. Editions Septima, Paris, 1980.
- <sup>15</sup>K. L. Scrivener and P. L. Pratt, "Characterisation of Portland Cement Hydration by Electron Optical Techniques"; pp. 351-68 in Electron Microscopy of Materials. Edited by W. Krakow, D. A. Smith, and L. W. Hobbs. Materials Research Society Symposium Proceedings, Vol. 31, 1983.
- <sup>16</sup>T. N. Tiegs, "Investigation of Ion-Thinned Tricalcium Silicate Pastes by Transmission Electron Microscopy"; M. Sc. Thesis, University of Illinois, Urbana-Champaign, 1975.
- <sup>17</sup>R. Javels, J. C. Maso, and J. P. Ollivier, "Realisation de lames ultra-mince de mortier pour observation directe au microscope electronique par transmission," *Cem. Concr. Res.*, 4, 167-76 (1974).
- <sup>18</sup>R. Javels, J. C. Maso, J. P. Ollivier, and B. Thenoz, "Observation directe au microscope electronique par transmission de la liaison pate de ciment-granulats de mortier de calcite et de quartz," *Cem. Concr. Res.*, 5, 285-94 (1975).



<sup>19</sup>B. J. Dalgleish, P. L. Pratt, and R. I. Moss, "Preparation Techniques and the Microscopical Examination of Portland Cement Paste and  $C_3S$ ," *Cem. Concr. Res.*, 10, 665-75 (1980).

<sup>20</sup>B. J. Dalgleish and K. Ibe., "Thin Foil Studies of Hydrated Portland Cement," *Cem. Concr. Res.*, 11, 729-39 (1981).

<sup>21</sup>K. L. Scrivener and P. L. Pratt, "Backscattered Electron Images of Polished Cement Sections in the Scanning Electron Microscope"; pp. 145-55 in Proceedings of the 6th International Conference on the Microscopy of Cements, International Cement Microscopy Association, 1984.

<sup>22</sup>K. L. Scrivener, H. H. Patel, P. L. Pratt, and L. J. Parrott, "Analysis of Phases in Cement Paste Using Backscattered Electron Images"; pp. 67-76 in Microstructural Development during Hydration of Cement. Edited by Leslie J. Struble and P. W. Brown. Materials Research Society Symposium Proceedings, Vol. 85, 1987.

<sup>23</sup>R. H. Bogue, *Ind. Eng. Chem. Analyt. Edn.*, 1 [4] 192 (1929).

<sup>24</sup>L. Struble, "A Review of Clinker Analysis by QXRD"; pp. 31-37 in Characterisation and Performance of Cement and Concrete. Engineering Foundation, New York, 1983.

<sup>25</sup>R. L. Berger, G. J. C. Frohnsdorff, P. H. Harris, and P. D. Johnson, "Application of X-Ray Diffraction to Routine Mineralogy Analysis of Portland Cement"; pp. 234-53 in Structure of Portland Cement Paste and Concrete. Highways Research Board SR90, 1966.

<sup>26</sup>W. A. Gutteridge, "Quantitative X-ray Powder Diffraction in the Study of Some Cementive Materials"; pp. 11-23 in Chemistry and Chemically Related Properties of Cement. Edited by F. P. Glasser. Proceedings of the British Ceramic Society, Vol. 35, 1984.

<sup>27</sup>K. L. Scrivener, "The Microstructure of Anhydrous Cement and its Effect on Hydration"; pp. 39-46 in Microstructural Development during Hydration of Cement. Edited by Leslie J. Struble and P. W. Brown. Materials Research Society Symposium Proceedings, Vol. 85, 1987.

<sup>28</sup>W. Gerhard and E. Nagele, "The Hydration of Cement Studied by Secondary Ion Mass Spectrometry (SIMS)," *Cem. Concr. Res.*, 13, 846-56 (1983).

<sup>29</sup>G. W. Groves, "Portland Cement Clinker Viewed by Transmission Electron Microscopy," *Cem. Concr. Res.*, 12, 619-25 (1982).

<sup>30</sup>K. L. Scrivener and P. L. Pratt, "Microstructural Studies of the Hydration of  $C_3A$  and  $C_4AF$  Independently and in Cement Paste"; pp. 207-20 in The Chemistry and Chemically Related Properties of Cement. Edited by F. P. Glasser. Proceedings of the British Ceramic Society, Vol. 35, 1984.

<sup>31</sup>D. Menetrier, I. Jawed, T. S. Sun, and J. Skalny, "ESCA and SEM Studies on Early  $C_3S$  Hydration," *Cem. Concr. Res.*, 9, 473-82 (1979).

<sup>32</sup>B. J. Dalgleish, P. L. Pratt, and E. Toulson, "Fractographic Studies of Early Hydration Products in Cement Paste," *J. Mater. Sci.*, 17, 2199-2207 (1982).

<sup>33</sup>B. J. Dalgleish, A. Ghose, H. M. Jennings, and P. L. Pratt, "The Correlation of Microstructures with Setting and Hardening in Cement Paste"; pp. 137-43 in International Conference on Concrete at Early Ages, Vol. 1, 1982.

<sup>34</sup>D. N. Hadley, "The Nature of the Paste-Aggregate Interface"; Ph.D. Thesis, School of Civil Engineering, Purdue University, West Lafayette, IN, 1972.

<sup>35</sup>P. L. Pratt and A. Ghose, "Electron Microscope Studies of Portland Cement Microstructures during Setting and Hardening," *Phil. Trans. R. Soc. (London), Sect. A*, 310, 93-103 (1983).

- <sup>36</sup>H. F. W. Taylor, "The Reactions of Cement Compounds with Water"; in Proceedings of the 10th International Symposium on the Reactivity of Solids, Dijon. Elsevier, Amsterdam, 1984.
- <sup>37</sup>K. L. Scrivener, "A Study of the Microstructure of Two Old Cement Pastes"; pp. 389-93 in Proceedings of the 8th International Congress on the Chemistry of Cement, Vol. III. Finep, Rio de Janeiro, Brazil, 1986.
- <sup>38</sup>H. Funk, "Two Different ways of Hydration in the Reaction of  $\beta$ - $\text{Ca}_2\text{SiO}_4$  with Water at 25 to 120°C"; pp. 291-95 in Proceedings of the 4th International Symposium on the Chemistry of Cement, Vol. I. Washington, National Bureau of Standards Monograph 43, 1962.
- <sup>39</sup>J. D. C. McConnell, "The Hydration of Larnite and Bredigite and the Properties of the Resulting Gelatinous Mineral Plomberite," *Mineral. Mag.*, 30, 672-80 (1955).
- <sup>40</sup>H. F. W. Taylor and D. E. Newbury, "An Electron Microprobe Study of a Mature Cement Paste," *Cem. Concr. Res.*, 14, 565-73 (1984).
- <sup>41</sup>K. L. Scrivener and H. U. Jensen; unpublished work.
- <sup>42</sup>A. Ghose and P. L. Pratt, "Studies of the Hydration Reactions and Microstructure of Cement Fly Ash Pastes"; pp. 82-91 in Proceedings of a Symposium on the Effects of Fly Ash in Cement and Concrete, Materials Research Society, Pittsburgh, 1981.
- <sup>43</sup>Y. Halse, D. Goult, and P. L. Pratt, "Calorimetry and Microscopy of Fly Ash and Silica Fume Cement Blends"; pp. 403-17 in The Chemistry of Chemically Related Properties of Cement. Edited by F. P. Glasser. British Ceramic Society, Stoke-on Trent, 1984.
- <sup>44</sup>Y. Halse, P. L. Pratt, J. A. Daziell, and W. A. Gutteridge, "Development of Microstructure and Other Properties in Fly Ash/OPC Systems," *Cem. Concr. Res.*, 14, 491-98 (1984).
- <sup>45</sup>H. Tanaka, Y. Totani, and Y. Saito, "Structure of Hydrated Glassy Blast Furnace Slag in Concrete"; pp. 963-77 in Proceedings of the 1st Conference on Fly Ash, Silica Fume, Slag, and Natural Pozzolans in Concrete, Vol. 2. Montebello, 1983.
- <sup>46</sup>A. M. Harrison, N. B. Winter, and H. F. W. Taylor, "An Examination of Some Pure and Composite Portland Cement Pastes using Scanning Electron Microscopy with X-ray Analytical Capability"; pp. 170-75 in Proceedings of the 8th International Congress on the Chemistry of Cement, Vol. IV. Finep, Rio de Janeiro, Brazil, 1986.
- <sup>47</sup>E. Dinsoy, T. Mosberg, and J. Young, "Influence of Aggregates on the Strength and Elastic Modulus of High Strength Mortars Containing Microsilica"; pp. 211-18 in Very High Strength Based Cement-Based Materials. Edited by J. Francis Young. Materials Research Society, Pittsburgh, 1985.
- <sup>48</sup>M. Regourd, "Microstructure of High Strength Cement Based Systems"; pp. 3-17 in Very High Strength Cement-Based Materials. Edited by J. Francis Young. Materials Research Society, Pittsburgh, 1985.
- <sup>49</sup>K. L. Scrivener and A. Bentur, "Quantitative Characterization of the Transition Zone in High Strength Concretes," *Adv. Cem. Res.*, 1 [4] 230-37 (1988).
- <sup>50</sup>B. B. Mandelbrot, *The Fractal Geometry of Nature*. W. H. Freeman & Co., New York, 1983.
- <sup>51</sup>D. N. Winslow, "The Fractal Nature of the Surface of Cement Paste," *Cem. Concr. Res.*, 15, 817-24 (1985).
- <sup>52</sup>L. Collis and R. A. Fox (eds.), "Aggregates: Sand, Gravel & Crushed Rock Aggregates for Construction Purposes"; Report of a Working Party of the Engineering Group of the Geological Society of London. The Geological Society, London, 1985.

- <sup>53</sup>B. D. Barnes, S. Diamond, and W. L. Dolch, "Micromorphology of the Interfacial Zone Around Aggregates in Portland Cement Mortar," *J. Am. Ceram. Soc.*, **62** [1] 21-24 (1979).
- <sup>54</sup>K. L. Scrivener and P. L. Pratt, "A Preliminary Study of the Microstructure of the Cement/Aggregate Bond in Mortars"; pp. 466-71 in Proceedings of the 8th International Congress on the Chemistry of Cement, Vol. III. Finep, Rio de Janeiro, Brazil, 1986.
- <sup>55</sup>J. Grandet and J. P. Ollivier, "Nouvelle methode d'etude des interface ciments-granulats"; pp. VII.85-89 in Proceedings of the 7th International Congress on the Chemistry of Cement, Vol. III. Editions Septima, Paris, 1980.
- <sup>56</sup>J. P. Ollivier, "Contribution a l'etude de l'hydratation de la pate de ciment portland au voisinage des granulats"; Thesis, L'Universite Paul Sabatier de Toulouse, France, 1981.
- <sup>57</sup>J. Grandet and J. P. Ollivier, "Orientation des hydrates au contact des granulats"; pp. VII.63-68 in Proceedings of the 7th International Congress on the Chemistry of Cement, Vol. II. Editions Septima, Paris, 1980.
- <sup>58</sup>P. J. M. Monteiro and P. K. Mehta, "Ettringite Formation on the Aggregate-Cement Interface," *Cem. Concr. Res.*, **15**, 378-80 (1985).
- <sup>59</sup>P. J. M. Monteiro, J. C. Maso, and J. P. Ollivier, "The Aggregate-Mortar Interface," *Cem. Concr. Res.*, **15**, 953-58 (1985).
- <sup>60</sup>L. Struble and S. Mindess, "Morphology of the Cement-Aggregate Bond," *Int. J. Cem. Comp. Lightw. Concr.*, **5**, 79-86 (1983).
- <sup>61</sup>J. Farran, "Contribution mineralogique a l'etude de l'adherence entre les constituants hydrates des ciment et les materiaux enrobes," *Rev. Mater. Construct.*, No. 490-491-492 (1956).
- <sup>62</sup>B. D. Barnes, S. Diamond, and W. L. Dolch, "The Contact Zone Between Portland Cement Paste and Glass 'Aggregate' Surfaces," *Cem. Concr. Res.*, **8**, 233-43 (1978).
- <sup>63</sup>P. J. M. Monterio and P. K. Mehta, "Interaction Between Carbonate Rock and Cement Paste," *Cem. Concr. Res.*, **16**, 127-34 (1986).
- <sup>64</sup>K. L. Scrivener and P. L. Pratt, "The Characterisation and Quantification of Cement and Concrete Microstructures"; pp. 61-68 in Pore Structure and Materials Properties, Vol. 1. Chapman & Hall, London, 1987.
- <sup>65</sup>K. L. Scrivener and E. M. Gartner, "Microstructural Gradients in Cement Paste Around Aggregate in Particles"; pp. 77-86 in Bonding In Cementitious Composites. Edited by S. Mindess and S. P. Shah. Materials Research Society, Pittsburgh.
- <sup>66</sup>K. L. Scrivener, A. K. Crumie, and P. L. Pratt, "A Study of the Interfacial Region Between Cement Paste and Aggregate in Concretes"; pp. 87-88 in Bonding in Cementitious Composites. Edited by S. Mindess and S. P. Shah. Materials Research Society Symposium Proceedings 114, Pittsburgh, 1988.
- <sup>67</sup>P. C. Kreijger, "The 'Skin' of Concrete Research Needs," *Mag. Concr. Res.*, **39**, [140] 122-23 (1987).
- <sup>68</sup>P. C. Kreijger, "The Skin of Concrete: Composition and Properties," *Mater. Construct.*, **17** [100] 275-83 (1984).
- <sup>69</sup>L. J. Parrott, "Measurement and Modelling of Moisture, Microstructure and Properties in Drying Concrete"; pp. 135-42 in Pore Structure and Materials Properties, Vol. 1. Chapman & Hall, London, 1987.
- <sup>70</sup>L. J. Parrott, D. C. Killoh, and R. G. Patel, "Cement Hydration under Partially Saturated Curing Conditions"; pp. 46-50 in Proceedings of the 8th International Congress of the Chemistry on Cement, Vol. III. Finep, Rio de Janeiro, Brazil, 1986.